ANALYTICA CHIMICA ACTA 608 (2008) 186–196

available at www.sciencedirect.com

ScienceDirect

journal homepage: www.elsevier.com/locate/aca

A miniature cytometry platform for capture and characterization of T-lymphocytes from human blood

He Zhu[a], *Monica Macal*[b], *Caroline N. Jones*[a], *Michael D. George*[b], *Satya Dandekar*[b], *Alexander Revzin*[a,*]

[a] *Department of Biomedical Engineering, University of California, Davis 95616, CA, United States*
[b] *Department of Medical Microbiology and Immunology, University of California, Davis 95616, CA, United States*

ARTICLE INFO

Article history:
Received 5 September 2007
Received in revised form
11 December 2007
Accepted 15 December 2007
Published on line 28 December 2007

Keywords:
Blood-based diagnostics
Antibody microarrays
Cell microarrays
T-cell capture

ABSTRACT

Given the clinical and diagnostic importance of blood analysis, there is considerable interest in developing novel miniature devices for rapid characterization of blood constituents. The present paper describes development of a miniature cytometry platform aimed at analysis of T-lymphocytes from peripheral human blood. Microarrays of T-cell-specific antibodies (Abs), including anti-CD3, -CD4, -CD8 and mouse IgG (negative control) were robotically printed onto glass slides coated with a non-fouling poly(ethylene glycol) (PEG) hydrogel. The glass substrates containing Ab arrays were incubated with 100 μL of red blood cell (RBC)-depleted whole human blood for 15 min and then exposed to a controlled shear of ~2 dyn cm^{-2} for additional 10 min. This process led to the removal of non-specific leukocytes and "development" of patterns of T-cells captured on the Ab spots. The immunofluorescent staining of the surface-bound cells revealed the presence of purified CD4$^+$ and CD8$^+$ T-cells (purity >94%) on their respective Ab spots. Importantly, the proportions of CD4$^+$ and CD8$^+$ T-cells captured on the Ab spots correlated closely (R^2 – 0.9) with flow cytometry analysis of T-cell subsets in blood. Overall, this cytometry platform allowed to rapidly (under 30 min) capture pure T-cell subsets from minimally processed human blood. Significantly, our device provided quantitative information about subset abundance solely based on the location of cells within the microarray. This cytometry platform is envisioned as a miniature immunology tool for determination of T-cell phenotype and will have immediate applications in HIV diagnostics and research.

1. Introduction

White blood cells or leukocytes are crucial participants in immunoprotection against pathogens. Variations in numbers of specific types of leukocytes commonly serve as indicators of infections, malignancies or autoimmune diseases [1]. For example, human immunodeficiency virus (HIV) causes depletion of CD4$^+$ T-lymphocytes in peripheral blood [2] and other lymphoid tissues (e.g. gastrointestinal mucosa) [3–5]. As a result, the absolute counts of CD4$^+$ T-cells and the ratio of CD4$^+$/CD8$^+$ T-lymphocytes are used as indicators of the onset of AIDS and as benchmarks for the initiation of antiviral therapy [6,7]. Other immune cells, including neutrophils and monocytes, commonly serve for disease diagnosis. For exam-

* *Corresponding author* at: Department of Biomedical Engineering, University of California, Davis, 451 East Health Sciences Street #2619, Davis, CA 95616, United States. Tel.: +1 530 752 2383; fax: +1 530 754 5739.
E-mail address: arevzin@ucdavis.edu (A. Revzin).
0003-2670/$ – see front matter © 2008 Elsevier B.V. All rights reserved.
doi:10.1016/j.aca.2007.12.021

ple, neutrophil counts have been closely associated with the level of inflammation in severely burned patients and those with coronary heart diseases [8].

Flow cytometry (FC) is the most commonly used leukocyte immunophenotyping method and is the "gold standard" for enumeration of T-lymphocytes in HIV-infected patients [9–11]. While FC is a robust technology that has proven invaluable for high-throughput, multiparametric characterization of leukocytes, it has several shortcomings. It is not well suited for monitoring individual cells over time; it limits morphology information to cell size and complexity, and requires a relatively large sample ($\sim 0.5 \times 10^6$ cells mL^{-1}) for analysis.

Compared to FC, immobilizing cells on the surface has a number of advantages including ease of monitoring over time and the possibility of analyzing cell morphology and function. The advantages of analyzing surface-bound cells have spurred the expansion of solid-phase cytometry—a field that focuses on analyzing cells affixed to glass slide [12,13]. The utility of solid-phase cytometry approaches can be greatly enhanced by miniaturizing leukocyte cytometry devices [14–16] and incorporating surface microfabrication approaches to organize leukocytes into spatially defined patterns [17–19]. Micropatterning of leukocyte-specific antibodies (Abs) has previously been employed to arrange leukocytes into high-density cell arrays enabling rapid cell screening and sorting [17–19]. However, surface micropatterning approaches derived from photoresist or soft lithography are not amenable to presenting several different Abs on the same surface, making multiplexed analysis of leukocyte populations difficult.

In contrast, robotic microarraying enables high-throughput printing of biomolecules on the same surface and has recently been employed to investigate cell-surface interactions in a multiplexed fashion [20–22]. In immunology research, robotic printing technology has been successfully utilized by Belov et al. to create cluster of differentiation (CD) Ab microarrays for multiplexed "panning" of leukocytes for immunophenotyping of leukemia [23–25]. More recently, Ab microarrays with individual spots containing cell- and cytokine-specific Abs for co-localized cell binding and cytokine release studies have been described [26].

While Ab microarrays have recently emerged as important leukocyte immunophenotyping tools, a number of technical challenges remain to be addressed. Arguably, the most important of these challenges is the ability to isolate pure leukocyte subsets from complex and heterogeneous samples such as whole blood. Isolating purified leukocyte subsets that accurately reflect proportions of leukocytes in peripheral blood will pave the way for quantitative, Ab microarray-based cytometry devices. Moreover, capture of specific sub-populations of leukocytes in different locations of the microarray will make these cells amenable to further phenotype and genotype analyses.

Importantly, despite a number of reports describing the use of Ab arrays for "panning" of leukocytes [23–26], we are not aware of studies aimed at capturing pure leukocyte subsets on Ab microarrays from whole blood in order to establish leukocyte subset proportions. For example, in their seminal paper, Belov et al. described leukocyte immunophenotyping on Ab arrays as a qualitative approach more suitable for characterizing population trends then providing quantitative information about subset proportions [23]. In other studies, Ab microarrays were employed to investigate leukocyte cell lines or primary T-cells that were purified prior to Ab microarray "panning" experiments [26].

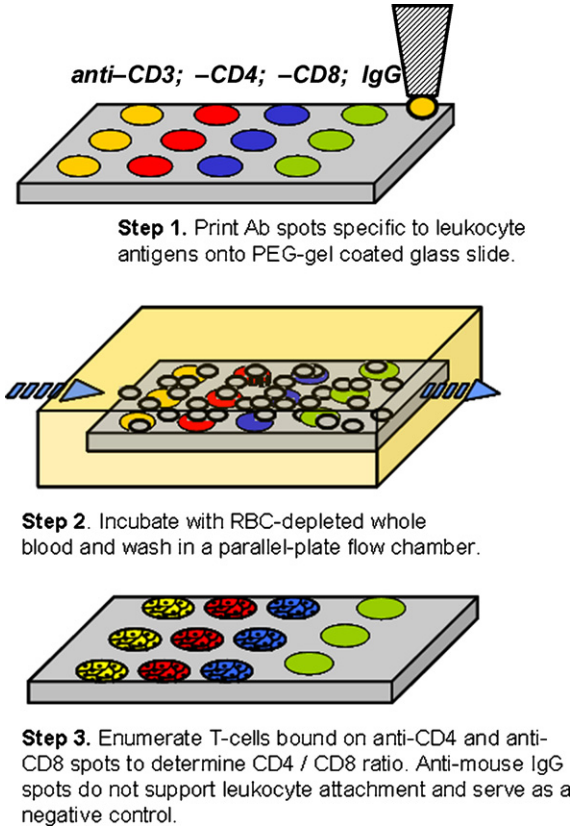

Fig. 1 – Schematic diagram experiments aimed at capturing T-cells on Ab microarrays and quantifying T-cell population proportions. *Step 1*: Arrays consisting of monoclonal mouse anti-human-CD3, -CD4, -CD8 and anti-mouse IgG (negative control) were printed onto PEG gel-coated glass slides. *Step 2*: Leukocyte suspension was incubated for 15 min at 4 °C with the Ab microarrays and washed in a parallel-plate flow chamber at a shear stress of ~2 dyn cm^{-2} for 10 min. *Step 3*: Washing resulted in appearance of cell microarrays comprised of $CD3^+$, $CD4^+$ and $CD8^+$ T-cells attached on their respective Ab spots. IgG Ab regions did not support leukocyte attachment and served as a negative control.

In contrast, the present paper investigated the utility of Ab microarrays for rapid capture of pure T-cell subsets from a complex cellular sample (peripheral blood) and for quantifying proportions of surface-bound leukocyte subsets (Fig. 1). Surface antigen-specific Abs (anti-CD3, anti-CD4 and anti-CD8) were robotically printed in replicates alongside the negative control spots (anti-mouse IgG) onto PEG gel-coated glass slides. A small volume (100 μL) of red blood cell (RBC)-depleted human blood was incubated with the Ab microarray for 15 min and washed under precisely defined shear flow (~2 dyn cm^{-2}) in a parallel-plate flow chamber for 10 min. Immunofluorescent labeling revealed that 94.7 ± 2.5% of human leukocytes captured on anti-CD4 Ab spots were $CD3^+CD4^+$ T-lymphocytes whereas 96.4 ± 1.2% of cells captured on anti-CD8 Ab spots

were $CD3^+CD8^+$ T-cells. Significantly, the proportions of $CD4^+$ and $CD8^+$T-cells bound to Ab spots correlated closely (R^2 – 0.9) to proportions of T-cells in blood determined by flow cytometry. The cytometry device described here served a dual purpose of (1) isolating pure T-cell subsets and (2) enumerating proportions of surface-bound T-cell subsets. This cytometry platform will have direct applications for monitoring dynamics of depletion, restoration and change of function in T-cells during HIV infections.

2. Materials and methods

2.1. Reagents

Paraformaldehyde (PFA), 10× phosphate-buffered saline (PBS) without calcium and magnesium, TWEEN 20, rabbit anti-mouse IgG antibody (2nd labeling antibody), EDTA, potassium bicarbonate ($KHCO_3$), ammonium chloride (NH_4Cl), poly(ethylene glycol) diacrylate (PEG–DA) (MW 575), anhydrous toluene (99.9%), sodium azide, bovine serum albumin (BSA), 0.1% poly-L-lysine, were acquired from Sigma–Aldrich (Saint Louis, MO). Purified mouse anti-human CD4 (13B8.2), anti-CD8 (B9.11) and anti-CD3 (×35) were employed as T-cell capture antibodies and were purchased from Beckman–Coulter (Fullerton, CA). Anti-mouse IgG2a (OX34) was purchased from Serotec Antibodies (Raleigh, NC). The following monoclonal antibodies were used for immunofluorescent labeling and were purchased from BD Pharmingen (San Diego, CA): mouse anti-human CD3ε-FITC (UCHT1), mouse anti-human CD4-PE (L120), mouse anti-human CD8-PE. Mouse anti-human monoclonal CD8–APC Cy5.5 antibodies and fetal bovine serum (FBS) were purchased from Invitrogen (Carlsbad, CA). Adhesion promoter, 3-acryloxypropyl trichlorosilane, was purchased from Gelest, Inc. (Morrisville, PA).

2.2. Printing of Ab microarrays

Glass surfaces were modified with 3-acryloxypropoyl trichlorosilane coupling agent and coated with poly(ethylene glycol) (PEG) gel according to the procedures reported earlier [27,28]. PEG gel-coated glass slides (75 mm × 25 mm) were dehydrated by lyophilization for 24 h and were stored in a dessicator prior to microarray printing. Purified mouse anti-CD4, -CD8 and -CD3 and mouse IgG2a (negative control) Abs were adjusted to concentration of 0.3 mg mL^{-1} in 1 × PBS. Ab microarrays were then printed onto dehydrated PEG gel-coated glass slides using GMS 417 Arrayer (Affymetrix, Santa Clara, CA) employing pins for printing 150 or 300 μm diameter spots. For printing experiments, 19 μL of dissolved Ab molecules were loaded into wells of a 384-well plate followed by the addition into each well of 1 μL of 0.1% TWEEN 20 surfactant. A typical printed array contained rows of anti-CD3, -CD4, -CD8 and anti-mouse IgG spots with 20 replicates per row (4 × 20 array). In addition to robotic microarrayer, a manual arrayer (MicroCaster, Schleicher & Schuell, Keene, NH) containing eight pins was used in the experiments. This system dispenses greater print volumes (20–70 nL compared to ∼1 nL for robotic arrayer) and forms larger (∼500 μm diameter) spots. This arraying system was used to print four Abs of interest with seven replicates (4 × 7 array). Immunofluorescent labeling was employed routinely to characterize morphology and quality of printed Ab spots. A small volume (∼200 μL) of 0.01 mg mL^{-1} anti-mouse IgG-FITC was incubated with Ab microarray for 30 min and then washed with copious amounts of 1× PBS. Immunostaining of Ab arrays were characterized by fluorescence microscopy.

2.3. Quantification of Ab molecules printed onto hydrogel-coated glass slides

Ab microarrays were printed onto PEG hydrogel-coated glass slides as described before and incubated in 1× PBS at 37 °C for 2 h. Ab molecules were extracted from PEG gel surface using 100 μL of 4 M guanidine–HCl (pH 7.2) supplemented with 0.2% 3-[(3-cholamidopropyl)-dimethylammonio]-1-propanesulfonate (CHAPS), 10 mM EDTA, 0.05 M Tris and protease inhibitor cocktail (Sigma–Aldrich, St. Louis, MO). The guanidine solution was incubated with the Ab microarray for 30 min. The supernatant was buffer-exchanged with 6 M urea containing 0.05 M Tris (pH 7.4) using Slide-A-Lyzer Mini Dialysis Units (Pierce) with 3500 MWCO for 1 h. The concentration of Ab extracted from the printed microarray was determined according to the manufacturer's instructions using Goat IgG ELISA Quantitation Kit (Bethyl Laboratories, Montgomery, TX).

2.4. Characterization of the effects of Ab concentration on cell capture

Mouse anti-human CD4 Ab was prepared with 0.005% (v/v) of TWEEN 20 in a range of concentrations, including: 0.20 mg mL^{-1}, 0.15 mg mL^{-1}, 0.10 mg mL^{-1}, 0.075 mg mL^{-1} and 0.050 mg mL^{-1}. Microarrays were robotically printed onto hydrogel-coated glass slides using solutions of varying Ab concentration. In order to determine whether solution concentration had an effect on density of Ab molecules entrapped in the hydrogel, the Ab microarrays were immunofluorescently labeled by incubation for 30 min with 0.01 mg mL^{-1} of goat anti-mouse IgG conjugated with Texas Red. DNA Microarray Scanner (Agilent Technologies, Santa Clara, CA) was used to image arrays of fluorescently labeled Ab spots. The scanner contained green (YAG laser – 532 nm wavelength) and red (He–Ne laser – 633 nm wavelength) channels and was used to scan standard 75 mm × 25 mm glass slides with 5 μm resolution. The fluorescence emanating from the printed protein spots was recorded in arbitrary intensity units and was used to establish a relationship between the Ab molecules immobilized in a hydrogel and the Ab solution concentration.

For quantifying efficiency of cell capture as a function of Ab concentration, anti-CD4 Abs were printed onto 75 mm × 25 mm hydrogel-coated glass slides. The following Ab printing solutions were prepared with 0.005% (v/v) Tween 20:0.20 mg mL^{-1}, 0.15 mg mL^{-1}, 0.10 mg mL^{-1}, 0.075 mg mL^{-1} and 0.050 mg mL^{-1}. Model T-lymphocytes (Jurkat cells) expressing CD4 antigen were used for quantifying cell capture dependence on the concentration of the Ab printing solution. Ab microarrays were incubated for 15 min with 2 mL volume of Jurkat cells at the concentration of 8×10^6 cells mL^{-1}. Then the slide was carefully transferred into the flow cham-

ber where the cells were subjected to a flow of 1× PBS at 0.8–2 dyn cm^{-2} for 5 min to ensure complete removal of non-specifically bound cells. The cells were then fixed with 4% PFA inside the flow chamber. Images of cells captured on Ab spots were obtained using a brightfield microscope. Cell density was determined by manually counting captured cells and normalizing by the area of the spot. A typical experiment represents an average cell density based six spots (~200 Jurkat cells per spot).

2.5. Blood sample preparation

In T-cell capture experiments; 3 mL of blood was collected from adult human subjects through venipuncture under sterile conditions with informed consent and approval of the Institutional Review Board of University of California, Davis (protocol number 200311635-6). The blood was mixed with 42 mL of erythrocyte lysis solution (89.9 g NH_4Cl, 10.0 g $KHCO_3$, and 370.0 mg tetrasodium EDTA in 10 L of deionized water) for 5 min at room temperature to lyse RBCs. The blood cell suspension was then centrifuged at 1000 rpm for 7 min. Lysed RBCs were dissolved in the suspension while leukocytes sedimented to the bottom. The supernatant was then decanted, and the leukocytes were re-suspended in 1× PBS to restore original volume of the blood sample. The cell suspension was immediately used for leukocyte panning experiments.

2.6. Capturing T-cells on Ab microarrays

The use of a parallel-plate fluidic chamber for capturing purified leukocyte subsets on Ab-decorated surfaces has been described by us previously [28]. In brief, a region of a glass slide containing Ab arrays was incubated (on ice) with 100 μL of RBC-lysed whole blood for 15 min. After incubating with cells, a glass slide was placed between two polycarbonate plates (50.8 mm × 127 mm × 6.35 mm (width × length × height)) of a custom built parallel-plate flow chamber [28,29] and secured with screws. Tubing was inserted into the chamber through inlet and outlet holes. A gasket with 100 μm depth was used to create and maintain an enclosed conduit between the upper plate and a glass slide. The effective dimensions of this conduit were 25.4 mm × 76.2 mm × 0.100 mm (width × length × height). Both plates had a glass window allowing for microscopy observation and leukocyte enumeration experiments to be performed *in situ*. The parallel-plate flow chamber created a uniform shear stress across the chamber as defined by the geometry of the chamber and input flow rate:

$$\tau = \frac{6\mu Q}{wh^2} \quad (1)$$

where τ is the uniform shear stress, μ is the viscosity of the flow, Q is flow rate, w and h refer to width and height of the chamber. Q was tuned to produce well-defined shear stress.

Cells residing on the surface were exposed to a flow rate of 500 μL min^{-1} (2 dyn cm^{-2} shear stress) created by an infuse/withdraw syringe pump PHD22/2000 (Harvard Apparatus, Holliston, MA). Removal of the cells was monitored by brightfield microscopy during washing to determine when the cell number on antibody spots stabilized. Typically, 10–15 min of washing was sufficient to remove non-specifically bound cells.

2.7. Immunophenotyping of T-cells captured on Ab microarrays

Leukocytes captured on Ab microarrays were identified by immunofluorescent staining. Anti-CD3-FITC and -CD4-PE or -CD8-PE were used to identify captured leukocytes as $CD3^+CD4^+$ and $CD3^+CD8^+$ cells. For immunostaining, the fluorescently labeled Abs were diluted 1/10 in 1× PBS containing 0.01% (w/v) BSA, mixed together and combined with nucleus-staining fluorophore—DAPI. The mixture of labeling molecules was then injected manually into the flow chamber and incubated with captured cells for 45–60 min in the dark at room temperature. After immunostaining, the flow chamber was flushed with 1× PBS at 500 μL min^{-1} for 10 min. Subsequently, 2% (w/v) PFA in 1× PBS was injected into the flow chamber to fix the cells *in situ* prior to removal of the T-cell array from the device.

For immunofluorescence imaging, the glass substrates containing leukocyte arrays were taken out of the chamber and observed using confocal microscope (Zeiss LSM 5 Pascal, Carl Zeiss, Inc.). The following excitation/emission settings were used for fluorescence imaging: FITC (488 nm/520 nm), PE (488 nm/575 nm) and DAPI (350 nm/461 nm). High-resolution images of the captured cell patterns were obtained using Hitachi S3500N scanning electron microscope (SEM) operating at 5 kV of accelerating voltage. For SEM imaging, cells captured on microarrays were sputter-coated with ~10 nm of Au–Pd.

Fluorescence images were used to determine the immunophenotype and purity of cells residing on specific Ab spots. Immunofluorescent labeling with anti-CD3-FITC and anti-CD4-PE or anti-CD8-PE was used to identify $CD3^+$, $CD3^+CD4^+$ and $CD3^+CD8^+$ T-cells. DAPI staining was used to determine nuclear morphology of cells and to evaluate non-specific binding to the Ab spots. For a typical experiment, multiple spots of each Ab/T-cell type (~2000 cells in total) were evaluated to determine an average purity of the three T-cell subpopulations. In addition to purity determination, T-cells residing on anti-CD4 and anti-CD8 Ab spots were enumerated to determine CD4/CD8 ratios. In a typical experiment, fifteen 150 μm diameter or five 500 μm diameter spots (~1000–2000 cells) of each Ab type were enumerated to determine T-cell proportions. The number of experiments was $n = 6$.

2.8. Flow cytometry analysis of T-cells

In order to validate T-cell subset proportions the flow cytometry analysis was carried out in parallel with enumeration of microarray-bound T-cells for each blood experiment. Lymphocytes from RBC-lysed whole blood were washed in 1mL 1× PBS 5 min at 1600 rpm, and pellets were re-suspended in staining buffer (filter sterilized 1× PBS with 3% heat-inactivated FBS and 0.1% sodium azide). Cells were incubated with fluorescent mouse anti-human monoclonal antibodies for CD3, CD8, and CD4 for 30 min at 4 °C. Anti-CD3-FITC, -CD4-PE and -CD8-APC Cy5.5 were used. Cells were then washed and fixed with 1% paraformaldehyde (PFA) prior to analysis on the LSR II flow cytometer (Beckton Dickinson (Mountain View, CA) at

the UC Davis core facility). A minimum of 500,000 events was collected for each sample and data was analyzed using Flow Jo (Tree Star, Inc. San Carlos, CA). $CD4^+$ and $CD8^+$ T-cells were determined by lymphocyte gate, doublet cell exclusion, and $CD3^+$ T-cell gate.

3. Results and discussion

The present paper describes development of an Ab microarray-based cytometry platform for rapid isolation and enumeration of $CD4^+$ and $CD8^+$ T-cells from a small volume of RBC-depleted human blood (Fig. 1). In addition to high purity (>94% for $CD4^+$ and $CD8^+$T-cells), the surface-bound cells accurately reflected CD4/CD8 subset proportions of whole blood. This miniature cytometry platform is envisioned as a novel tool of diagnostics and monitoring of HIV/AIDS or other diseases associated with modulation of leukocyte numbers and function.

3.1. *Printing of Ab microarrays*

A typical Ab microarray used in our experiments contained leukocyte antigen-specific anti-CD3, -CD4, -CD8 Abs as well as anti-mouse IgG Abs serving as negative control (Fig. 1). Robotically printed microarrays (150 or 300 μm diameter spots) consisted of four capture Abs printed in 19 replicates (4 × 20 array) whereas manually printed arrays (500 μm diameter spots) contained 4 × 7 members. Prior to printing, PEG gel-coated glass slides were dehydrated using lyophilization to ensure rapid incorporation of Ab molecules into the gel. After printing, glass substrates were re-hydrated to create a non-fouling PEG gel matrix around imprinted Ab domains.

Studies were undertaken to evaluate effectiveness of PEG hydrogel coating to serve as a matrix for immobilization of Ab molecules. In these studies, microarrays of a model mouse IgG Ab (alpha1-anti-trypsin) were robotically printed onto hydrogel-coated as well as silane-coated glass slides. Modification of glass substrates with acryloxypropyl trichlorosilane resulted in silane layer with thickness of ~5 nm and a contact angle of ~60°. The silanized glass surfaces were compared to glass substrates coated with 5–10 μm thick layer of cross-linked hydrogel composed of small molecular weight (MW – 575) PEG chains. Upon printing Ab microarrays, the glass substrates were incubated in 1× PBS at 37 °C for 2 h and then exposed to guanidine-based protein extraction buffer. Antibody quantification ELISA kit was then employed to quantify the concentration of Ab molecules extracted from microarrays. Given that the quantification protocol was based on calibration curves and required a significant amount of Abs, we employed a model mouse IgG (apha1-anti-trypsin) that was considerably less expensive than anit-CD4 Ab. Because the isotype for both antibody molecules was the same, the results presented here are directly applicable to binding of anti-CD4 Ab. The data presented in Fig. 2 demonstrate that a hydrogel-coated glass substrate contained ~60% more Ab molecules per unit area compared to a silanized surface. This result points to increased surface area for Ab binding offered by the hydrogel coating compared to the silanized glass substrate. The Ab density on hydrogel and silane-treated glass slides was 1.7 and 1.06 ng mm^{-2}, respectively compared to an ideal value of 2.85 ng mm^{-2}. This ideal surface density was approximated by assuming that the Ab solution (0.2 mg mL^{-1}) was printed on the surface in a 1 nL volume, forming a 300 μm diameter spot. While the actual Ab density on a hydrogel-coated substrate was found to be 60% of the ideal value. The efficiency of the guanidine extraction protocol in removing proteins immobilized in a matrix is ~70% and may account, in large part, for the discrepancy between the actual and the ideal Ab surface densities. In addition, Ab molecules might have dissociated from the gel during incubation of the microarrays. The results presented in Fig. 2 indicate that the majority, if not all, of the robotically printed Ab molecules became incorporated into the PEG hydrogel matrix. In contrast, considerably lower Ab density was achieved on a two-dimensional glass substrate modified with only a silane layer.

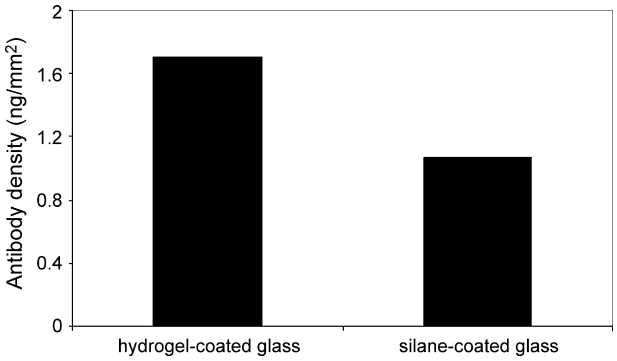

Fig. 2 – Quantifying efficiency of Ab binding onto the substrate after printing. In these experiments, a model mouse IgG Ab (alpha1-anti-trypsin) was printed in 8 × 10 array of 300 μm diameter spots. Guanidine extraction protocol, used to remove Ab molecules from printed microarrays, was followed by ELISA analysis to determine concentration of the extracted Ab molecules. The ideal scenario where 100% of printed Ab molecules remain on the surface was estimated to be 2.85 ng mm^{-2}. The actual Ab surface density, after 2 h incubation in 1 × PBS at 37 °C, was determined to be 1.7 and 1.06 ng mm^{-2} for hydrogel- and silane-coated glass substrates, respectively. Therefore, the Ab surface density on the hydrogel-coated glass substrate was approaching that of the ideal scenario. The Ab density values reported here may represent maximal binding capacity of a hydrogel-coated surface. However, the difference between the ideal value and the Ab surface density on PEG hydrogel coating may also be explained by the efficiency of guanidine-based protein extraction protocol, estimated to be around 70%.

Experiments were also carried out to determine Ab solution concentration leading to the highest on-the-spot density of captured T-lymphocytes. In these experiments, different anti-CD4 Ab solutions ranging in concentration from 0.05 to 0.2 mg mL^{-1} were prepared and printed onto hydrogel-coated glass slides. Immunofluorescent staining of the Ab

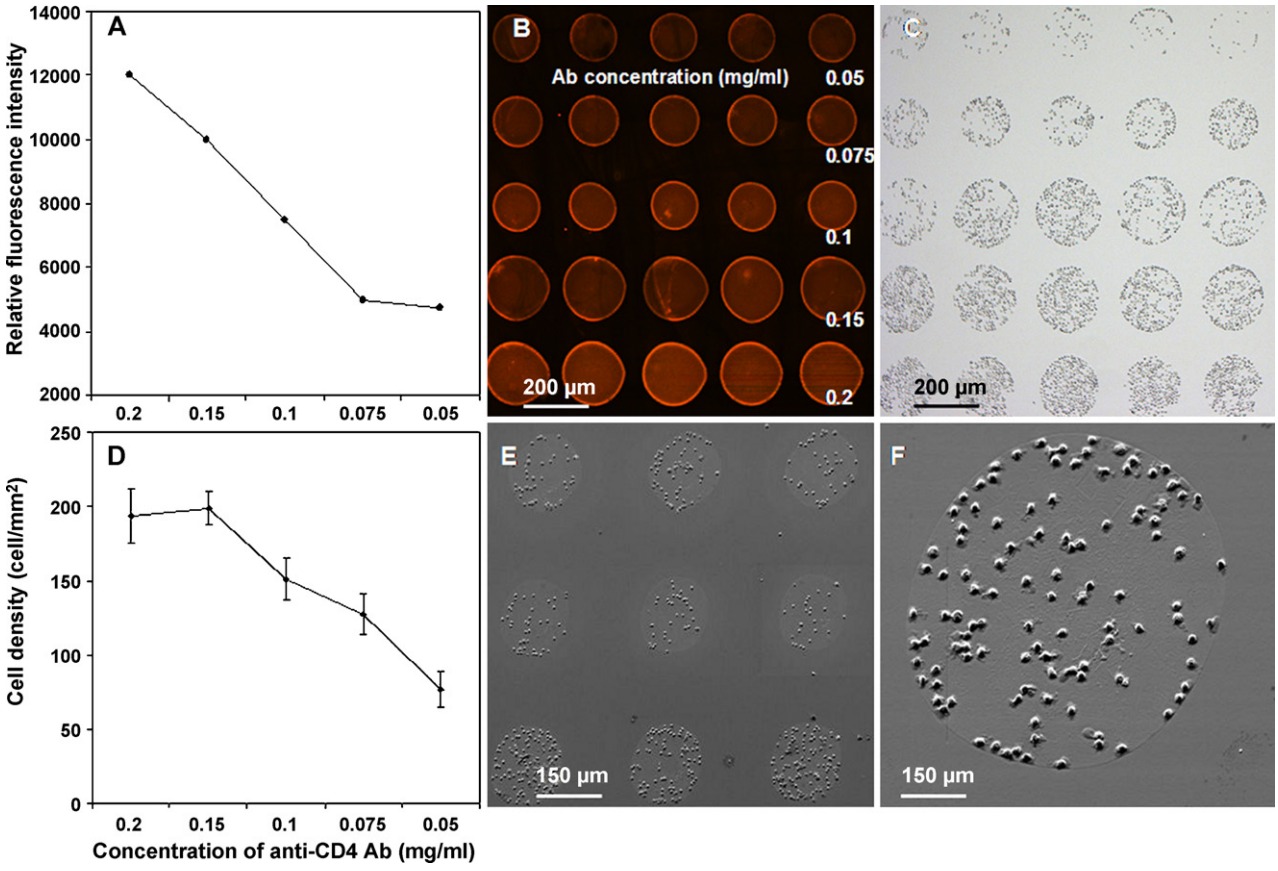

Fig. 3 – (A and B) Mouse anti-human CD4 Ab molecules were printed at different concentrations onto a hydrogel coated slide and then immunostained with goat anti-mouse IgG Texas Red. (A) Fluorescence intensity readout obtained from the array scanner and (B) corresponding fluorescence image. (C and D) Model lymphocytes (Jurkat cells) attaching to anti-CD4 Ab spots printed at different concentrations. (C) Brightfield image (40× magnification) of cells captured on Ab spots printed at different concentration and (D) cell density analysis demonstrating dependence of cell capture on Ab concentration. (E) SEM micrographs of Ab microarrays after incubation with RBC-depleted whole blood showing capture of small and rounded cells morphologically consistent with lymphocyte phenotype. Each row corresponds to a different capture Ab: top – anti-CD4, middle – anti-CD8, bottom – anti-CD3. Variation in the numbers of cells attached to different Ab spots reflects proportions of T-cell subsets in whole blood. (F) Higher magnification (400×) SEM micrograph of a single anti-CD4 Ab spot with immobilized $CD4^+$ T-cells. (For interpretation of the references to color in this figure legend, the reader is referred to the web version of the article.)

spots and incubation with CD4 antigen-expressing model T-lymphocytes (Jurkat cells) were then employed to identify the solution concentration leading to optimal Ab incorporation and cell capture. For immunostaining experiments, arrays of mouse anti-human CD4 Ab spots printed from different concentrations of Ab stock solution were incubated with anti-mouse IgG Ab conjugated with Texas Red. A microarray scanner was used to determine relative fluorescence intensity of spots. As demonstrated by Fig. 3A, the fluorescence signal emanating from printed Ab spots decreased as a function of Ab stock solution concentration. It should be noted that 0.2 mg mL^{-1} was "as received" concentration of anti-CD4 Ab therefore; a higher concentration could not be obtained without concentrating (e.g. by lyophilization) and reconstituting the Ab solution. Fig. 3B demonstrates an immunofluorescent image of a microarray where each row of spots corresponds to different Ab stock solution concentration. This fluorescence image corroborates the Ab concentration-dependent decrease in the spot intensity described in Fig. 3A. These results indicate that the Ab solution concentration was indeed a key determinant of on-the-spot density of Ab molecules and that the use of high concentration of Ab printing solution (0.2 mg mL^{-1}) was necessary to create spots with high Ab density. One should note that the results presented in Fig. 3(A and B) point to efficient immobilization of Ab molecules into the PEG hydrogel coating. As seen from Fig. 3A, a 25% decrease in solution concentration from 2 to 1.5 mg mL^{-1} led to considerable loss of immunofluorescence. This once again underscores that a large fraction of printed Ab molecules became incorporated into the hydrogel matrix, even at high Ab solution concentration. These results corroborate ELISA data presented in Fig. 2.

Importantly, as seen from Fig. 3B, labeling Abs employed for immunofluorescent staining interacted exclusively with printed spots, highlighting the non-fouling properties of the surrounding PEG gel layer. As described in the following

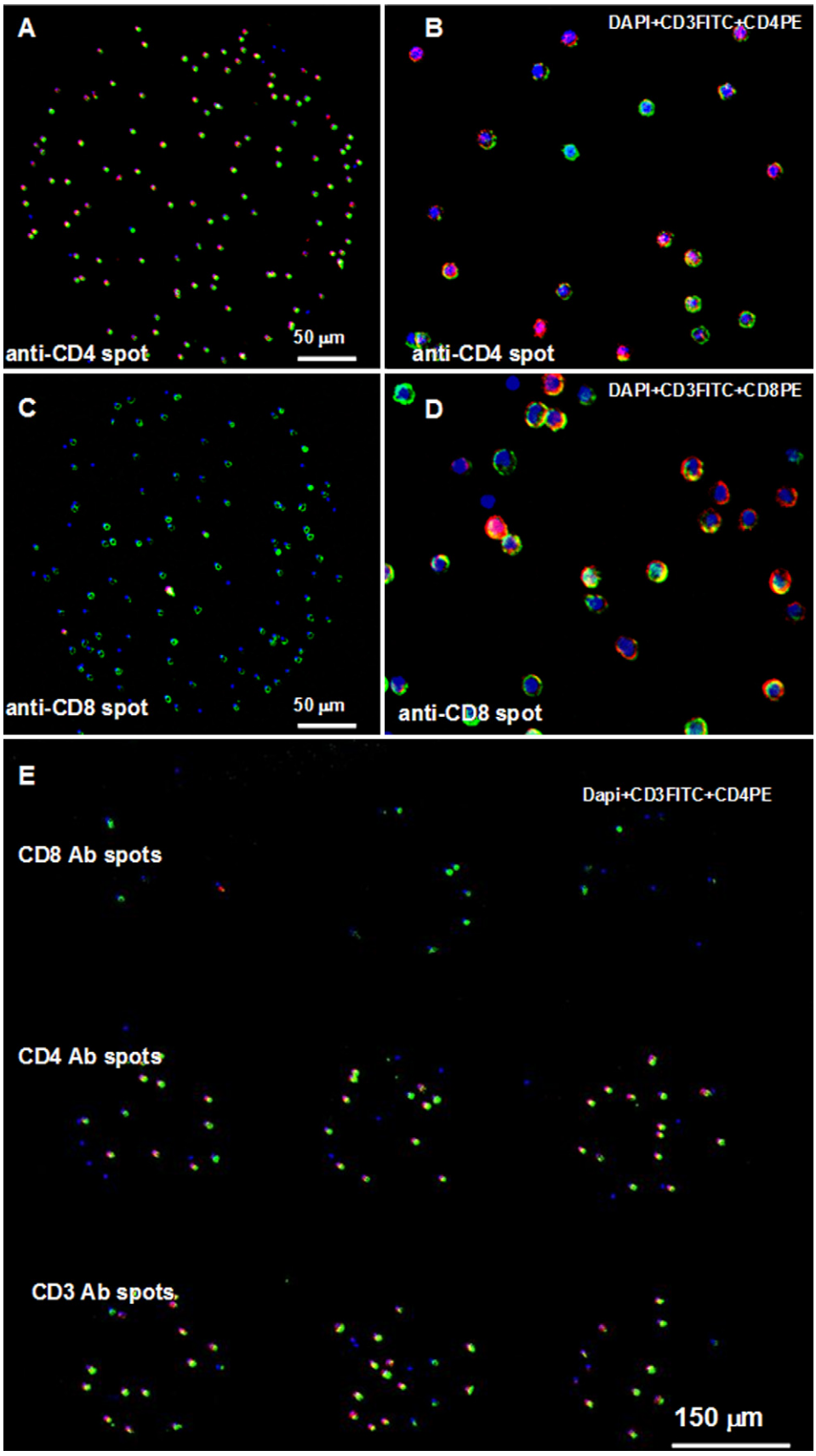
A
anti-CD4 spot
50 μm
B
DAPI+CD3FITC+CD4PE
anti-CD4 spot
C
anti-CD8 spot
50 μm
D
DAPI+CD3FITC+CD8PE
anti-CD8 spot
E
Dapi+CD3FITC+CD4PE
CD8 Ab spots
CD4 Ab spots
CD3 Ab spots
150 μm

section, leukocytes showed similar specificity in binding to printed Ab spots.

3.2. *Capturing T-lymphocytes on Ab microarrays*

Upon incubating leukocytes with printed Ab microarrays, surfaces were washed at a well-defined flow rate in a parallel-plate flow chamber. In our previous study, we found it important to employ a specific shear stress range where loosely, non-specifically bound leukocytes are removed without dislodging selectively captured cells [28]. This shear stress window was determined to be from 0.8 to 2 dyn cm^{-2}, corresponding to flow rates ranging from 200 to 500 $\mu L\,min^{-1}$ for our flow chamber geometry. Comparable shear stress values were previously demonstrated to be optimal for isolation of model leukocytes and primary T-cells in microfluidic devices [14–16].

After exposure to leukocyte suspension, Ab microarray was completely covered with cells (images not shown); however, upon initiation of flow at a defined shear stress, arrays of T-cells emerged (see Fig. 3C for example). Removal of loosely bound cells from Ab spots was monitored by brightfield microscopy to determine the time required for achieving stable cell numbers. Typically this occurred after 10 min of washing. After washing, the PEG gel regions surrounding Ab domains remained free of cells, pointing to excellent anti-fouling properties of this surface coating.

As mentioned in the previous section, we carried out experiments aimed at determining the effects of the Ab solution concentration on Ab immobilization and T-cell capture on PEG hydrogel-coated glass slides. Fig. 3(C and D) demonstrates the results of an experiment where model T-lymphocytes (Jurkat cells) were incubated with an array of anti-CD4 spots printed from stock solutions of varying Ab concentration. As seen from Fig. 3C, on-the-spot cell density was directly proportional to the Ab solution concentration, with the exception of two highest concentrations (0.15 and 0.2 $mg\,mL^{-1}$) were saturation in cell density was observed. Quantification of cell capture density as a function of Ab solution concentration, presented in Fig. 3D, corroborated visual evidence of an image shown in Fig. 3C. Interestingly, while fluorescence intensity and on-the-spot Ab density was higher for 0.2 $mg\,mL^{-1}$ compared to 0.15 $mg\,mL^{-1}$ stock Ab solution concentration (Fig. 3A), no significant difference in on-the-spot density was observed. This is likely due to entrapment of some of the Ab molecules within the hydrogel matrix, making them inaccessible for binding with T-cell surface antigens. The results presented in Fig. 3(C and D) once again underscore the importance of the Ab concentration of the printing solution for ensuring efficient capture of T-cells.

Table 1 – Summary of six separate experiments aimed at investigating purity of T-lymphocyte subsets captured on their respective Ab spot

Experiment (#)	Purity of T-cells bound on Ab microarrays		
	$CD3^+$ (anti-CD3 spots) (%)	$CD3^+CD4^+$ (anti-CD4 spots) (%)	$CD3^+CD8^+$ (anti-CD8 spots) (%)
1	na	96.0 ± 3.2	99.0 ± 0.7
2	95.8 ± 1.0	96.7 ± 1.0	95.9 ± 0.4
3	97.4 ± 1.4	94.6 ± 0.9	95.6 ± 3.4
4	92.6 ± 2.4	91.7 ± 4.0	96.6 ± 4.0
5	97.2 ± 1.4	91.2 ± 3.1	96.3 ± 1.9
6	97.7 ± 2.4	98.0 ± 1.5	95.4 ± 5.4
Average	96.1 ± 1.9	94.7 ± 2.5	96.4 ± 1.2

Immunofluorescent staining was used to determine T-cell purity. In each experiment, cells residing on multiple spots of the same Ab type were evaluated using fluorescence microscopy to calculate an average value for each T-cell subset.

Fig. 3E shows an SEM micrograph of T-cells captured on anti-CD4 spots (upper row), anti-CD8 spots (middle row) and anti-CD3 spots (bottom row). As seen from this image, the abundance of T-cells residing on Ab domains varied, with anti-CD3 spots containing the most cells, anti-CD8 domains being least populated and the anti-CD4 spots containing an intermediate number of cells. Given that both $CD4^+$ and $CD8^+$ T-cells express CD3 antigen, T-cell abundance on the anti-CD3 Ab spots is expected. As seen from a higher magnification micrograph in Fig. 3F, an anti-CD4 Ab spot contained small and circular cells—morphology consistent with that of lymphocytes. Immunofluorescence and flow cytometry experiments presented in the following sections revealed that the differences in T-cell subset abundance observed on Ab microarrays in Fig. 3E faithfully reflected T-cell subset proportions of peripheral blood.

Fig. 4 – T-lymphocytes bound onto several antigen-specific Abs printed in an array of 500 μm or 150 μm diameter spots. Cells were immunolabeled with anti-CD3-FITC (green), anti-CD4-PE (red) or anti-CD8-PE. Nucleus-staining fluorophore DAPI (blue) was used to assess nuclear morphology. Importantly, very few cells residing on anti-CD3, anti-CD4 and anti-CD8 Ab spots were stained with DAPI only, pointing to limited non-specific cell attachment. (A) Human T-cells captured on 500 μm diameter anti-CD4 Ab spot (100×). (B) A higher magnification fluorescence image (400×) acquired from the same Ab spot showing that captured T-cells stained positive for CD3 antigen (FITC-green) as well as for CD4 antigen (PE-red). The $CD3^+CD4^+$ phenotype clearly identifies captured cells as $CD4^+$ T-cells. (C and D) Tri-color fluorescence image of cells immobilized on a 500 μm diameter anti-CD8 spot demonstrates that captured cells were $CD3^+CD8^+$ pointing to $CD8^+$ T-cell phenotype. (E) Capture of cells onto microarrays comprised of anti-CD3, -CD4, -CD8 and -mouse IgG Abs. Immunofluorescent labeling with anti-CD3-FITC/anti-CD4-PE/DAPI revealed that $CD3^+$, $CD3^+CD4^+$ and $CD3^+CD4^-(CD8^+)$ T-cells were residing on their respective spots within the Ab microarray (100×). The numbers of cells captured on CD4 vs. CD8 Ab spots were counted to calculate CD4/CD8 T-cell ratio. (For interpretation of the references to color in this figure legend, the reader is referred to the web version of the article.)

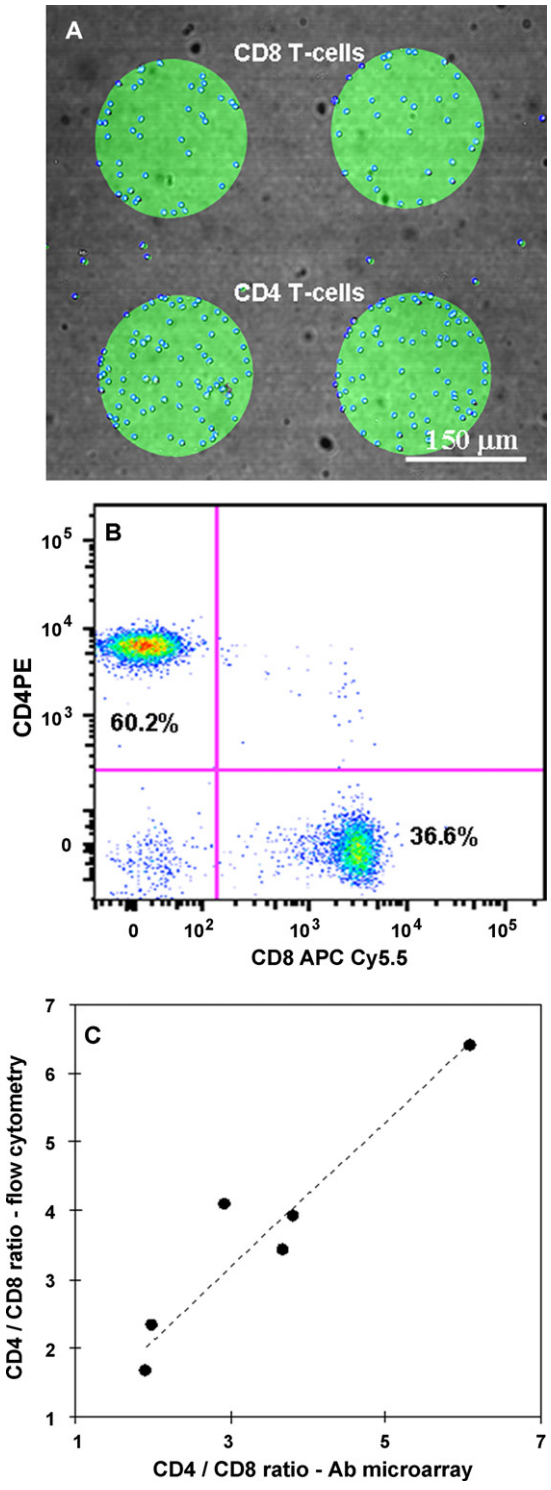

Fig. 5 – Comparing T-cell proportions determined by Ab microarrays vs. flow cytometry. (A) An image demonstrating T-cells captured on anti-CD4 and anti-CD8 spots were stained with DAPI (blue) while printed Ab spots were immunostained with anti-mouse IgG-FITC (green). Simple counting of $CD4^+$ and $CD8^+$ T-cells residing on their respective Ab spots was used to determine CD4/CD8 ratio. (B) Typical flow cytograms from RBC-lysed blood sample. Lymphocyte population determined by forward and side scatter was gated to single cells and then further gated to $CD3^+$ T-cell population while the proportions of $CD4^+$ and $CD8^+$ T-cells were determined within a CD3 gate. Flow cytometry was performed in parallel and with the same blood samples used in Ab microarray experiments. (C) Comparison of CD4/CD8 ratio estimated from Ab microarrays and flow cytometry shows close correlation (R^2 – 0.9) between the two approaches. Results from six separate experiments were compared. (For interpretation of the references to color in this figure legend, the reader is referred to the web version of the article.)

3.3. *Immunofluorescent staining to determine phenotype of captured T-cells*

For immunophenotype determination, captured cells were stained with fluorescent Abs as shown in Fig. 4. CD3 is a ubiquitous T-lymphocyte antigen common to both $CD4^+$ and $CD8^+$ T-cells, therefore, fluorescent Abs for CD3, CD4 and CD8 antigens were used to determine captured cells as double positive $CD3^+CD4^+$ or $CD3^+CD8^+$ T-lymphocytes. Importantly, care was taken to select different clones of labeling and capturing anti-CD3, -CD4 and -CD8 Abs in order to avoid competitive binding to the same epitope of leukocyte antigen. In addition to fluorescently labeled Abs, nuclear stain DAPI was used to determine nuclear morphology of the captured cells.

Fig. 4 (A–D) demonstrates typical tri-color fluorescence images of T-cells bound on Ab domains. As seen from Fig. 4(A and B) the majority of cells captured on anti-CD4 Ab spot stained positive for both CD3 antigen (FITC-green) and CD4 antigen (PE-red) with all cells being stained with DAPI (blue). The $CD3^+CD4^+$ phenotype identifies captured cells as $CD4^+$ T-lymphocytes. Importantly, none of the cells shown in Fig. 4(A and B) were stained with DAPI only, pointing to lack of non-specific cell binding. Similarly, immunofluorescent staining of cells bound to anti-CD8 Ab spots (Fig. 4(C and D)) revealed majority of the cells to be positive for CD3 (green) and CD8 (red) antigens, pointing to $CD3^+CD8^+$ phenotype of these T-cells.

Fig. 4E shows a representative cell microarray with T-cells captured on anti-CD3, -CD4 and CD8 Abs printed side-by-side. Another row of spots, consisting of mouse-IgG Ab domains served as a negative control for the experiments and was typically void of cells (not shown here). The immunofluorescence images presented in Fig. 4E demonstrate that cells captured on the three rows of Ab spots were positive for CD3 antigen (green) while only those cells bound to anti-CD4 and anti-CD3 spots stained positive (red) for CD4 antigen. This is reasonable given that $CD3^+CD8^+$ T-lymphocytes in general do not express CD4 antigen. Overall, the data presented in Fig. 4E, demonstrate successful capture of purified $CD4^+$ and $CD8^+$ T-lymphocytes in the same microarray.

Importantly, while CD4 antigen is expressed on monocytes as well as T-lymphocytes, small rounded DAPI-stained nuclei of cells bound on anti-CD4 Ab spots (see Fig. 4B) were consistent with lymphocyte nucleus morphology. No cells with large irregularly shaped nuclei resembling monocytes were observed on anti-CD4 Ab spots. These results are corroborated by our previous findings showing lack of monocyte retention on anti-CD4-decorated gel surfaces [28]. Exposure

of surface-bound cells to a well-defined shear stress is a key parameter for removal of contaminating monocytes. Cheng et al. recently demonstrated that exposure of cells bound on anti-CD4 surfaces to a shear stress range of 1–2 dyn cm^{-2} effectively eliminated monocytes but did not dislodge surface-bound $CD4^+$ T-cells [14]. Therefore, our washing conditions (~2 dyn cm^{-2}) likely serve as an added filter in removing contaminating monocytes from printed anti-CD4 domains.

To analyze purity of captured T-lymphocytes, cells residing on Ab arrays were counted and scored as either $CD3^+CD4^+$ or $CD3^+CD8^+$ using fluorescence microscopy. Cells residing on multiple spots of the same Ab type were counted to calculate an average purity value for each T-cell type for a given experiment. The results from six separate experiments compiled in Table 1 reveal consistently high purity of $CD3^+$ (96.1 ± 1.9%), $CD4^+$ (94.7 ± 2.5%) and $CD8^+$ (96.4 ± 1.2%) T-lymphocyte subsets isolated on their respective Ab spots. Ensuring the high-purity of desired T-cell subsets bound on the surface is an important pre-requisite to quantitative determination of subset proportions. In the next set of experiments, the relative abundance of $CD4^+$ and $CD8^+$ T-cells bound on Ab microarrays was compared to T-cell subset proportions of whole blood.

3.4. *Determining T-cell proportions with Ab microarrays*

Determining population proportions of $CD4^+$ and $CD8^+$ T-cells is an important component of leukocyte immunophenotyping. For example, during HIV infections, $CD4^+$ T-cells in peripheral blood are depleted while the level of $CD8^+$ T-cells remains constant. Therefore, in addition to absolute counts of $CD4^+$ T-cells, the CD4 to CD8 ratio is commonly monitored in HIV infections.

In the present study, the proportions of $CD4^+$ and $CD8^+$ T-cells captured on the Ab microarrays were compared to flow cytometric analysis of T-cell subsets in RBC-depleted blood. Fig. 5A demonstrates anti-CD4 and anti-CD8 spots containing human T-lymphocytes. In this experiment the Ab spots were immunofluorescently labeled with anti-mouse IgG-FITC (green) while T-lymphocytes were stained with DAPI to underscore the localization of cells on the Ab domains. As seen from this image, the relative abundance of cells captured on anti-CD4 and anti-CD-8 Abs differed considerably, with $CD4^+$ cells being on average two to six times more abundant than $CD8^+$ cells. For each experiment, the number of T-cells residing on anti-CD4 and -CD8 Ab spots was counted to calculate CD4/CD8 ratio. In parallel to isolation of T-cells on Ab microarrays, RBC-depleted blood samples were analyzed by flow cytometry to determine T-cell population proportions in peripheral blood using this standard immunophenotyping technology. Fig. 5B demonstrates flow cytometry data from one blood experiment which determined 60% of cells within the CD3 (T-cell) gate to be $CD4^+$ and 36% to be $CD8^+$, yielding the CD4/CD8 ratio of 1.7. For the same blood experiment, the enumeration of cells bound on Ab microarrays provided a CD4/CD8 ratio of 1.9. A comparison of CD4/CD8 subset proportions from six separate experiments, compiled in Fig. 5C, shows close correlation (R^2 − 0.9) between Ab microarray-based and flow cytometry-based enumeration.

These data are highly significant, as they highlight potential utility of Ab microarrays for quantitative immunophenotyping of leukocytes. Importantly, consistently high purity of T-cells isolated on specific Ab domains, underscored by the data in Table 1, eliminates the necessity of performing immunofluorescent staining for each leukocyte "panning" experiment. Instead, T-cell subset proportions may be determined by brightfield microscopy observation of specific domains within the cell microarray. While helping enumerate population proportions of leukocytes in blood, this "location" gating significantly simplifies immunophenotyping, paving the way for inexpensive immunology diagnostics devices.

4. Conclusions

In this paper, we describe the development of a cytometry platform employing robotically printed Ab microarrays for rapid capture and characterization of T-cells from whole human blood. Immunofluorescent staining experiments revealed that cells bound on Abs specific to CD3, CD4 and CD8 antigens were $CD3^+$, $CD4^+$ and $CD8^+$ T-lymphocytes with purity exceeding 94% for each subset. Significantly, the proportions of $CD4^+$ and $CD8^+$ T-cells bound on Ab spots correlated closely (R^2 − 0.9) to T-cell proportions in whole blood as determined by flow cytometry. Importantly, the leukocyte capture and characterization required a small sample volume (<100 μL) and took less than 30 min to complete.

The ability to quantify leukocyte subsets solely based on the "location" gating is a particularly powerful feature of Ab microarrays as it may obviate the need for fluorescently labeled Abs and drastically decrease the cost of such immunological assays as HIV testing. Capturing multiple pure leukocyte populations onto the same substrate from whole blood also opens possibility of multiplexed interrogation of immunogenic potential of these cells. Upon interrogation, leukocytes of interest may be retrieved (sorted) from the cell microarray for downstream analysis using laser capture microdissection techniques [19,30]. Similarly, isolating pure leukocyte subsets in a location-specific fashion may allow identifying cytokine profile of the cells, and thus, provide additional phenotype and cell function information. It should be noted that while the present platform focuses on phenotyping of T-lymphocytes, other immune cells, including neutrophils and monocytes have been captured using Ab microarrays [28]. Neutrophil counts have been closely associated with the level of inflammation in severely burned patients and those with coronary heart diseases [8]. Therefore, Ab microarray-based cytometry device may be a useful tool for monitoring an inflammatory response based on enumeration and functional analysis of neutrophils.

Overall, Ab microarray-based cytometry platform described here is envisioned as a central component of a miniature device for isolation, enumeration and interrogation of leukocytes.

Acknowledgements

We thank Prof. Louie's lab in the Department of Biomedical Engineering at UC Davis for providing assistance with

confocal microscopy. Technical advice provided Dr. David Verhoeven is greatly appreciated. In addition, we thank Dr. Kazuhiko Sekine, Department of Emergency & Critical Care Medicine, Saiseikai Yokohamashi Tobu Hospital, Yokohama, Japan for the technical advice concerning leukocyte panning experiments. This publication was supported in part by the California Research Center for the Biology of HIV in Minorities, California HIV/AIDS Research Program #CH05-D-606. HZ was supported through an NIH fellowship grant (EB003827).

REFERENCES

[1] M.L. Turgeon, Clinical Hematology, 3rd ed., Lippincott Williams & Wilkins, 1999.
[2] R.F. Siliciano, T. Lawton, C. Knall, R.W. Karr, P. Berman, T. Gergory, E.L. Reinherz, Cell 54 (1988) 561–575.
[3] Z. Smit-McBride, J.J. Mattapallil, M. McChesney, D. Ferrick, S. Dandekar, J. Virology 72 (1998) 6646–6656.
[4] R.S. Veazey, M. DeMaria, L.V. Chalifoux, D.E. Shvetz, D.R. Pauley, H.L. Knight, M. Rosenzweig, R.P. Johnson, R.C. Desrosiers, A.A. Lackner, Science 280 (1998) 427–431.
[5] R.S. Veazey, P.S. Marx, A.A. Lackner, Trends Immunol. 11 (2001) 626–633.
[6] J. Guarner, P. Montoya, C. del Rio, G. Hernandez-Tepichin, Cytometry 30 (1997) 178–180.
[7] G.G. Sherman, J.S. Galpin, J.M. Patel, B.V. Mendelow, D.K. Glencross, J. Immunol. Methods 222 (1999) 209–217.
[8] M. Madjid, I. Awan, J.T. Willerson, S.W. Casscells, J. Am. Coll. Cardiol. 44 (10) (2004) 1945–1956.
[9] M. Bergeron, S. Faucher, T. Ding, S. Phaneuf, F. Mandy, Cytometry 50 (2002) 62–68.
[10] B. Brando, D. Barnett, G. Janossy, F. Mandy, B. Autran, G. Rothe, B. Scarpati, Cytometry 42 (2000) 327–346.
[11] I. Storie, A. Sawle, K. Goodfellow, L. Whitby, V. Granger, R.Y. Ward, J. Peel, T. Smart, J.T. Reilly, D. Barnett, Cytometry B 57B (2004) 47–52.
[12] E. Bedner, P. Burfeind, W. Gorczyca, M.R. Melamed, Z. Darzynkiewicz, Cytometry 29 (1997) 191–196.
[13] R.J. Clatch, J.R. Foreman, Cytometry 34 (1998) 36–38.
[14] X.H. Cheng, D. Irimia, M. Dixon, K. Sekine, U. Demirci, L. Zamir, R.G. Tompkins, W. Rodriguez, M. Toner, Lab Chip 7 (2) (2007) 170–178.
[15] S.K. Murthy, A. Sin, R.G. Tompkins, M. Toner, Langmuir 20 (2004) 11649–11655.
[16] A. Sin, S.K. Murthy, A. Revzin, R.G. Tompkins, M. Toner, Biotechnol. Bioeng. 91 (2005) 816–826.
[17] H. Kim, R.E. Cohen, P.T. Hammond, D.J. Irvine, Adv. Mater. 16 (2006) 1313–1323.
[18] H. Kim, J. Doh, D.J. Irvine, R.E. Cohen, P.T. Hammond, Biomacromolecules 5 (2004) 822–827.
[19] A. Revzin, K. Sekine, A. Sin, R.G. Tompkins, M. Toner, Lab Chip 5 (2005) 30–37.
[20] C.J. Flaim, S. Chien, S.N. Bhatia, Nat. Methods 3 (2005) 119.
[21] D.G. Anderson, S. Levenberg, R. Langer, Nature Biotechnol. 22 (2004) 863–866.
[22] A. Revzin, P. Rajagopalan, A.W. Tilles, F. Berthiaume, M.L. Yarmush, M. Toner, Langmuir 20 (2004) 2999–3005.
[23] L. Belov, O. de la Vega, C.G. dos Remedios, S.P. Mulligan, R.I. Christopherson, Cancer Res. 61 (2001) 4483–4489.
[24] L. Belov, P. Huang, J.S. Chrisp, S.P. Mulligan, R.I. Christopherson, J. Immunol. Methods 305 (2005) 10–19.
[25] Y. Soen, D.S. Chen, D.L. Kraft, M.M. Davis, P.O. Brown, PLoS Biol. 1 (2003) 429–438.
[26] D.S. Chen, Y. Soen, T.B. Stuge, P.P. Lee, J.S. Weber, P.O. Brown, M.M. Davis, PLoS Med. 2 (2005) 1018–1030.
[27] A. Revzin, R.G. Tompkins, M. Toner, Langmuir 19 (2003) 9855–9862.
[28] K. Sekine, A. Revzin, R.G. Tompkins, M. Toner, J. Immunol. Methods 313 (2006) 96–109.
[29] A.W. Tilles, H. Baskaran, P. Roy, M.L. Yarmush, M. Toner, Biotechnol. Bioeng. 73 (2001) 379–389.
[30] J.Y. Lee, C.N. Jones, M.A. Zern, A. Revzin, Anal. Chem. 78 (2006) 8305–8312.